Rare Metal Materials and Engineering
Volume 52, Issue 6, June 2023
Available online at www.rmme.ac.cn

Science Press

Cite this article as: Xu Hui, Guo Yanjun, Wang Jiangwei, et al. Degradation Behavior of Microstructures and Mechanical Properties of GTD111 Turbine Blade After Long-Term Service[J]. Rare Metal Materials and Engineering, 2023, 52(06): 2057-2062.

ARTICLE

Degradation Behavior of Microstructures and Mechanical Properties of GTD111 Turbine Blade After Long-Term Service

Xu Hui[1,2], Guo Yanjun[1], Wang Jiangwei[2], Wang Lu[1], Li Xiaohui[1], Qiao Lijie[1], Qiu Zhibin[1]

[1] Materials Research Center, Huadian Electric Power Research Institute Co., Ltd, Hangzhou 310030, China; [2] School of Materials Science and Engineering, Zhejiang University, Hangzhou 310027, China

Abstract: The evolution of microstructures and mechanical properties stimulated by long-term service was investigated using a GTD111 blade employed in the first stage rotor blade of a heavy-duty gas turbine. Results show that the microstructures of the blade are mainly composed of γ matrix, γ' precipitates with two dimensions, $\gamma+\gamma'$ eutectic and *M*C-type carbides. The microstructural degradation of the blade is closely related to its structural characteristics. Samples from leading edge and middle region of the blade exhibit a relatively lower degree of microstructural degradation, while samples from trailing edge of the blade possess higher degree of microstructural degradation. The ultimate tensile strength (UTS) of the leading edge region is significantly higher than that of the trailing edge region at room temperature, but the UTS of different regions has little difference at 982 °C, which may be related to different deformation mechanisms at higher temperatures.

Key words: turbine blade; microstructure; γ' precipitate; carbide; mechanical property

Nickel-based superalloys are widely used in heavy-duty gas turbine blades due to their good high temperature strength, creep resistance, thermal corrosion resistance and oxidation property[1–2]. The excellent performance of superalloy is derived from its special chemical compositions and microstructures. On the one hand, strong solid solution strengthening effect will be provoked by adding plenty of refractory elements into γ matrix[3–5]. On the other hand, precipitation strengthening can be obtained by the formation of coherent γ' precipitates in γ substrate and *M*C-type or $M_{23}C_6$-type carbides, which hinder the movement of dislocations and grain deformation and thus strengthen the alloy[6–9]. However, with the diffusion and redistribution of alloying elements, the degradation of γ' precipitates and the decomposition of carbides proceed continuously due to the environment of high temperature gas erosion, high frequency vibration, centrifugal stress and alternating thermal stress, and microstructure properties of superalloy will be deteriorated, leading to the decrease in service performance[10–13].

There have been a large number of studies on the microstructure degradation of nickel-base superalloys under different experimental parameters, such as coating degradation and shedding, coarsening and rafting of γ' phase, TCP precipitation, carbide decomposition and grain boundary (GB) coarsening[14–16]. In the actual service process, the evolution mechanism of blades is extremely complex due to the interaction of temperature, stress, corrosion and other factors[17].

Usually the test rods prepared in laboratory was used to study the underlying mechanisms of microstructural evolution in serviced turbine blades[18–20]. While, in this study, the first-stage rotor blade of PG9171E gas turbine employed in a gas power plant for about 27 000 h (equivalent operating hours), was selected as the sample to analyze the evolution behavior of microstructure and mechanical property after long-term service, so as to provide theoretical basis for performance assessment and defect diagnosis of service blades.

1 Experiment

Microstructural examination and mechanical tests were

Received date: September 01, 2022
Corresponding author: Xu Hui, Ph. D., Senior Engineer, Materials Research Center, Huadian Electric Power Research Institute Co., Ltd, Hangzhou 310030, P. R. China, E-mail: hui-xu@chder.com

carried out on the blade, which is made of GTD111 Ni-based superalloy, using traditional equiaxial crystal casting process. Its nominal compositions are shown in Table 1. As shown in Fig. 1, the overall external structure of selected blade can be classified into three parts, i.e., blade body, platform and root, with 11 cooling holes inside. In order to study the differences in the underlying mechanisms of microstructure evolution caused by the inhomogeneity of service conditions, typical test blocks were cut along radial direction at tip, middle, root and tenon of the blade, labeled as S1−S4, respectively. For S1 to S3 blocks located at the blade body, further machining was taken out along the axial direction of the blade, in order to obtain the samples of leading edge (LE), middle side (MS) and trailing edge (TE).

Microstructural observation was performed using Hitachi SU-70 scanning electron microscope (SEM) equipped with energy dispersive spectrometer (EDS). Metallographic specimens were ground by SiC abrasive paper and polished, then chemically corroded for 5−15 s with an etchant solution including 4 g $CuSO_4$+20 mL HCl+20 mL H_2O. Tensile tests were completed using 50 kN CMT-5504 electronic universal testing machine. The tensile strain was controlled by chuck displacement with a constant deformation rate of 0.57 mm/min and testing temperatures of 25 and 982 °C. In view of the reliability of testing data, two samples were tested for each experimental condition at least.

2 Results and Discussion

2.1 Microstructure evolution induced by long-time service

Typical fluctuation in microstructure morphology of cross-section of specimen S1, due to inhomogeneity of service conditions, is depicted in Fig. 2. It can be found that grain boundary (GB), $\gamma+\gamma'$ eutectic, larger intergranular carbides and smaller transgranular carbides exist in the γ matrix of LE under lower magnification (Fig. 2a). Further observation shows that γ' precipitates possess hierarchical dimensions, including larger size of primary γ' and smaller size of secondary γ' (Fig. 2b). Though transgranular carbides maintain block-shape without evident degradation, intergranular carbides are inclined to decompose, forming aggregated fine particles. On the both sides of GBs, narrow γ' depleted trunnels are generated due to the accelerated diffusion of alloying elements at the GBs. At the region of MS, the macrostructural configuration is composed of γ matrix, γ' precipitates with two hierarchical dimensions, carbides, and $\gamma+\gamma'$ eutectic, which keep a relatively good shape, showing no prominent appearance of aging features (Fig. 2c). However, local region with aging features can be captured near the GBs, which include coarsening and depleting of γ' precipitates as shown in Fig. 2d. With the decrease in thickness of the blade, the cooling capacity of cooling holes is weakened gradually, which will accelerate the microstructural degradation. It can be inferred from Fig. 2e that γ' precipitates of TE region are coarsened obviously after long-time service in contrast with other regions. Besides the γ' precipitates, blocky carbides at inner grains transform into spherical shape that embraces γ' lamellae, and γ' depleted region forms around GBs with the absence of primary γ'.

Comparing the microstructural morphology of three sites in specimen S1, it can be found that the discrepancy of aging degree between LE and MS is quite negligible. So further microstructural observation is mainly focused on the LE and TE regions. The typical microstructural morphology of LE area in specimen S2 is depicted in Fig. 3a and 3b, where the primary γ' precipitates adjacent to GBs tend to dissolve and are replaced by fine secondary γ' precipitates, forming γ' depleted region. Nevertheless, the γ' precipitates far away from GBs underdo a coarsening process, exhibiting evident increase in γ' precipitate size. The *M*C carbides are found to keep good condition without apparent decomposition actions at the intergranular or transgranular regions. Higher magnification observation reveals that a plenty of secondary γ' precipitates are embedded on the coarsened primary γ' particles. At the TE area of specimen S2, the coarsening of γ' precipitates becomes more obvious, which occurs not only in primary γ' precipitates, but also in secondary γ' precipitates, forming a complex hollow structure (Fig. 3c). The coarsened primary γ' precipitates and secondary γ' precipitates interact at the interfaces, and grow up towards each other (Fig. 3d). However, the *M*C carbides of TE area have no obvious change in morphology features as well.

The microstructural variation of specimen S3 at different

Table 1 Chemical compositions of tested gas turbine blade

C	Cr	Co	Al	Ti	W	Mo	Ta	Zr	B	S	P	Ni
0.09	13.95	9.78	3.10	4.85	4.08	1.47	2.60	0.006	0.012	0.005	0.004	Bal.

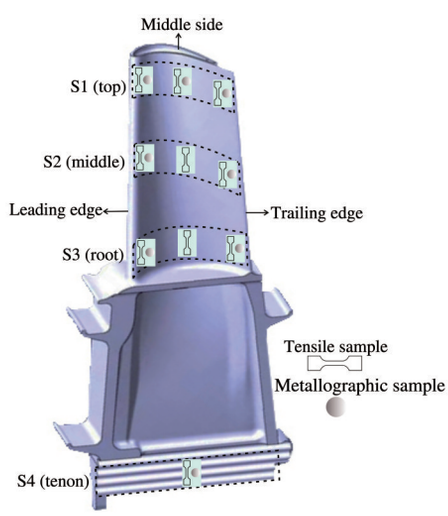

Fig.1 Schematic diagram of blade macrostructure and sampling plan

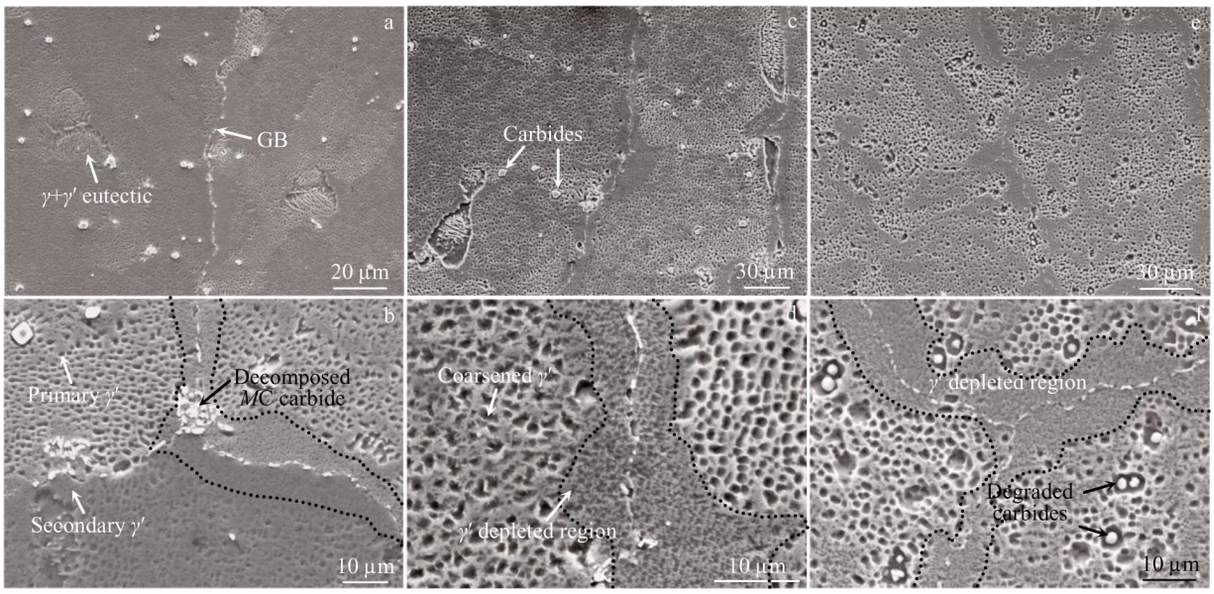

Fig.2 Typical microstructures of specimen S1 at different positions: (a–b) LE, (c–d) MS, and (e–f) TE

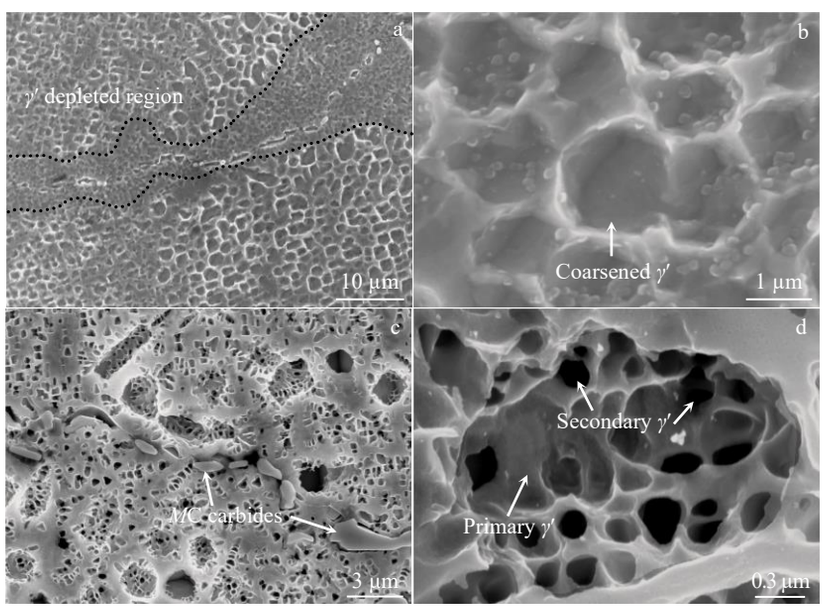

Fig.3 Typical microstructures of specimen S2 at different positions: (a–b) LE and (c–d) TE

regions is exhibited in Fig. 4. The most prominent characteristics of microstructure degradation in this part is reflected by the morphological evolution of γ' precipitate and GB, while no strong clues are found, proving the constituent phase modification and *M*C carbide degradation in comparison with other sites. At the LE side, most of the primary γ' precipitates are obviously coarsened and turn into spherical shape. At the TE side, apart from the depleted region near GBs, rafted primary γ' precipitates at inner grains can also be found, which nearly rearrange along the same direction.

The typical microstructures of tenon specimen S4 and original specimen cut from an blade not in service are shown in Fig. 5. Due to lower service temperature and stress, microstructural degradation of tenson specimen is relatively weaker compared to other specimens. Apart from $\gamma + \gamma'$ eutectic, blocky carbides without obvious degradation are observed at the dendrite region of tension specimen (Fig. 5a). The γ' precipitates near GBs are ellipsoidal or blocky and uniformly distributed in γ matrix, and meanwhile γ' depleting is even absent from GB affected zone (Fig. 5b). However, for the blade not in service, *M*C-typed carbides embed along GBs in a good condition, duplex γ' precipitates including rectangular primary γ' and fine secondary γ' are evenly distributed in the face centered cubic γ matrix (Fig.5c and 5d).

2.2 Tensile behavior affected by temperatures and sampling locations

The variation curves of tensile property for samples

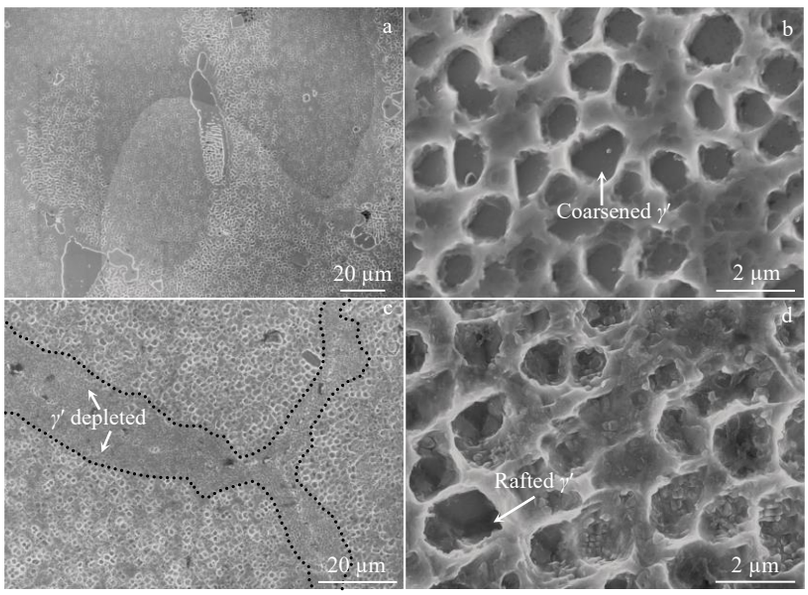

Fig.4 Typical microstructures of specimen S3 at different positions: (a–b) LE and (c–d) TE

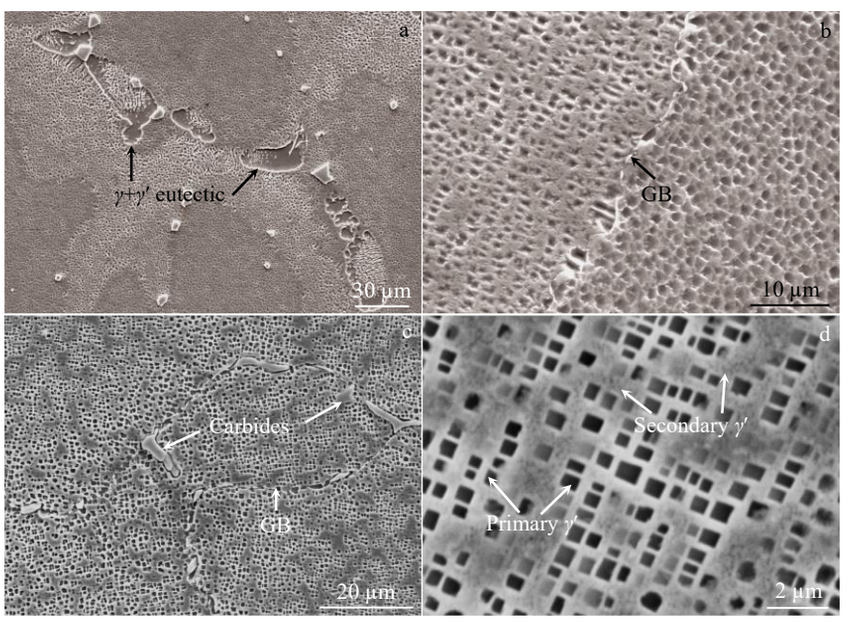

Fig.5 Microstructural comparison between tenon specimen S4 (a–b) and original specimen (c–d): (a) interdendrite region, (b) dendrite region, (c) GBs, and (d) duplex γ' precipitates

deformed at room temperature are shown in Fig.6a, where the UTS and elongation of contrast new blade specimens are 1185 MPa and 8.2%, respectively. From the horizontal comparisons of UTSs for samples at tip, middle and root, it can be found that on the LE side, the UTS of blade tip is the highest, followed by the middle and root of blade that are close to each other. On the MS side, equivalent UTSs are found at the tip and middle of blade, and lower UTS is detected at the root of blade. On the TE side, UTS at blade tip is the lowest, while UTSs at the other two sites are higher and comparable. By the vertical comparisons of UTSs between different samples, it is proved that the UTS of LE side is generally higher than that of TE side. With respect to elongation, the variation trends of the LE and TE specimens are similar to the change of corresponding UTSs at the same sampling sites, i.e. increasing or decreasing initially, and then being stable. However, the variation trends of the MS specimens seem to be opposite to UTS, exhibiting a certain inversion relationship. Further comparative analysis shows that the aging degree of the microstructure in TE region is greater than that of LE region, which weakens local mechanical properties, resulting in much lower UTS of TE than that of LE region.

The variation curves of tensile properties for samples deformed at 982 °C are shown in Fig. 6b, and the UTS and

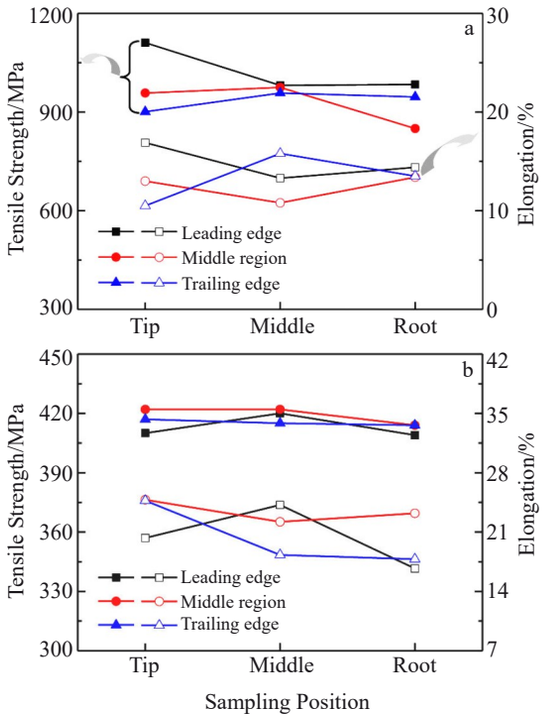

Fig.6 Mechanical properties of tensile specimens sampled from different positions of turbine blade: (a) RT and (b) 982 ℃

elongation of contrast new blade specimens are 499 MPa and 26.3%, respectively. It can be revealed from the horizontal comparisons that the UTSs of tip, middle and root specimens are nearly the same, with a maximal fluctuation value of 15 MPa, no matter where the specimens were sampled. Similarly, it is proved by vertical comparisons that the UTSs of LE, MS and TE specimens with respective sampling sites varying from blade tip to blade root are nearly the same too, i. e. the fluctuation values are all less than 15 MPa. A relatively large gap is discovered for the changes of elongation of the specimens sampled from the blade tip to blade root that have different tendencies in the change of final elongation. Further comparison shows that the influence of microstructure on tensile properties is weakened at the higher temperature.

It is implied by the above results that obvious discrepancy in the behavior of microstructure evolution and mechanical performance is produced in different regions of the served turbine blade. Due to the relatively larger thickness and well cooling effect at LE and MS regions, the microstructure aging of the blade is characterized by γ' coarsening, γ' depleting near GBs and intergranular *M*C carbide decomposition, which suggest lower degree of aging extent. However, the aging extent at TE region is significantly aggravated on account of the smaller thickness and much weaker cooling effect, which results in the occurrence of degraded intragranular *M*C carbide embedded by γ' lamellae, and the ripened or nearly rafted γ' precipitates. According to the tensile curves at room temperature, the UTS of the TE area is apparently lower than that of the LE area, which indicates that the microstructure aging of the blade can significantly accelerate the degradation of mechanical properties. Nevertheless, when the testing temperature is increased up to 982 °C, the differences of UTS at different positions decrease significantly, and all of them change in a very narrow range, revealing weaker dependence of UTS on the aged microstructures in the blade. This can be attributed to the modified deformation mechanisms at different temperatures[21–22]. When tensile deformation occurs at RT, anti-phase boundary shearing and stacking fault shearing dominate the original plastic strain, and flow stress is greatly affected by the resistance of γ' precipitates to shear[23]. However, when deformed at 982 °C, plastic strain is mainly accommodated by individual matrix dislocations bypassing γ' precipitates, leading to the decreased dependence of flow stress on γ' precipitates[24–25].

3 Conclusions

1) The microstructures of tested turbine blade are mainly composed of γ matrix, γ' precipitates with two dimensions, γ+γ' eutectic and *M*C-type carbides.

2) Samples at leading edge (LE) and middle side (MS) exhibit a relatively lower degree of microstructural degradation, while samples from trailing edge (TE) region show higher degree of microstructural degradation.

3) UTS of the LE region is significantly higher than that of the TE region at room temperature, while there is little difference in the UTS of different regions at 982 °C, which may be related to different deformation mechanisms at higher temperatures.

References

1 Wen M Y, Sun Y, Yu J J *et al*. *Journal of Alloys and Compounds*[J], 2020, 835: 155 337
2 Pollock T M. *Nature Materials*[J], 2016, 15: 809
3 Zhang X M, Deng H Q, Xiao S F *et al*. *Computational Materials Science*[J], 2013, 68: 132
4 Heckl A, Neumeier S, Göken M *et al*. *Materials Science and Engineering A*[J], 2011, 528: 3435
5 Rae C M F, Reed R C. *Acta Materialia*[J], 2001, 49: 4113
6 Ola O T, Ojo O A, Chaturvedi M C. *Materials Science and Engineering A*[J], 2013, 585: 319
7 Zhao Y S, Zhang J, Luo Y S *et al*. *Acta Materialia*[J], 2019, 176: 109
8 Liu T, Cheng X N, Luo R *et al*. *Materials Science and Engineering A*[J], 2021, 819: 1
9 Zhao K, Ma Y H, Lou L H. *Journal of Alloys and Compounds*[J], 2009, 475: 648
10 Lvova E. *Journal of Materials Engineering and Performance*[J], 2007, 16: 254
11 Qin X Z, Guo J T, Yuan C *et al*. *Materials Science and Engineering A*[J], 2008, 485: 74
12 Lou X M, Sun W R, Guo S R, *et al*. *Rare Metal Materials and Engineering*[J], 2008, 37(2): 259 (in Chinese)
13 Song X X, Zhou L, Li K *et al*. *Rare Metal Materials and*

Engineering[J], 2021, 50(10): 3427
14 Lvov G, Levit V I, Kaufman M J. *Metallurgical and Materials Transactions A*[J], 2004, 35A: 1669
15 Wang X G, Li J R, Liu S Z *et al*. *Rare Metal Materials and Engineering*[J], 2017, 46(3): 646
16 Miura N, Nakata K, Miyazaki M *et al. Materials Science Forum*[J], 2010, 638–642: 2291
17 Mazur Z, Luna Ramírez A, Juárez Islas J A *et al. Engineering Failure Analysis*[J], 2005, 12: 474
18 Du B N, Yang J X, Cui C Y *et al. Materials Science and Engineering A*[J], 2015, 623: 59
19 Xu H, Zhang Z J, Zhang P *et al. Scripta Materialia*[J], 2017, 136: 92
20 Yang Y H, Xie Y J, Wang M S *et al. Materials & Design*[J], 2013, 51: 141
21 Chu Z K, Yu J J, Sun X F *et al. Materials Science and Engineering A*[J], 2010, 527: 3010
22 Zhang P, Yuan Y, Li B *et al*. *Materials Science and Engineering A*[J], 2016, 655: 152
23 Zhang P, Yuan Y, Shen S C *et al*. *Journal of Alloys and Compounds*[J], 2017, 694: 502
24 Liu J L, Yu J J, Jin T *et al*. *Transactions of Nonferrous Metals Society of China*[J], 2011, 21: 1518
25 Fan Z D, Wang C C, Zhang C *et al*. *Materials Science and Engineering A*[J], 2018, 735: 114

重型燃气轮机透平GTD111叶片长期服役后微观组织与性能退化行为

许　辉[1,2]，郭延军[1]，王江伟[2]，王　鲁[1]，郦晓慧[1]，乔立捷[1]，邱质彬[1]
(1. 华电电力科学研究院有限公司 材料研究中心，浙江 杭州 310030)
(2. 浙江大学 材料科学与工程学院，浙江 杭州 310027)

摘　要：研究了某重型燃气轮机透平第一级GTD111动叶片经长期服役后的微观组织和力学性能演变行为。结果表明，服役叶片的微观组织主要由γ基体、2种尺寸的γ'相、γ+γ'共晶及*M*C型碳化物组成。叶片的微观组织退化与其结构特性密切相关。叶片前缘和中部区微观组织退化程度相对较轻，而叶片后缘区微观组织退化更为严重。在室温下，叶片前缘区抗拉强度明显高于尾缘区，然而在982 ℃下不同区域的抗拉强度相差不大，可能与高温下的变形机制不同有关。

关键词：透平叶片；微观组织；γ'相；碳化物；力学性能

作者简介：许　辉，男，1987年生，博士，高级工程师，华电电力科学研究院有限公司材料研究中心，浙江 杭州 310030，E-mail：hui-xu@chder.com